Dalton Transactions

ROYAL SOCIETY OF CHEMISTRY

PAPER

View Article Online
View Journal | View Issue

Cite this: *Dalton Trans.*, 2020, **49**, 15779

Tuning Rh(II)-catalysed cyclopropanation with tethered thioether ligands†

Derek Cressy, Cristian Zavala, Anthony Abshire, William Sheffield and Ampofo Darko *

Received 28th August 2020,
Accepted 26th October 2020

DOI: 10.1039/d0dt03019h

rsc.li/dalton

Dirhodium(II) paddlewheel complexes have high utility in diazo-mediated cyclopropanation reactions and ethyl diazoacetate is one of the most commonly used diazo compounds in this reaction. In this study, we report our efforts to use tethered thioether ligands to tune the reactivity of Rh^{II}-carbene mediated cyclopropanation of olefins with ethyl diazoacetate. Microwave methods enabled the synthesis of a family of Rh^{II} complexes in which tethered thioether moieties were coordinated to axial sites of the complex. Different tether lengths and thioether substituents were screened to optimise cyclopropane yields and minimise side product formation. Furthermore, good yields were obtained when equimolar diazo and olefin were used. Structural and spectroscopic investigation revealed that tethered thioethers changed the electronic structure of the rhodium core, which was instrumental in the performance of the catalysts. Computational modelling of the catalysts provided further support that the tethered thioethers were responsible for increased yields.

1. Introduction

Dirhodium(II) paddlewheel (Rh^{II}) complexes have become ubiquitous in carbene chemistry since the Teyssié group first demonstrated that they were capable of decomposing diazo compounds (Fig. 1).[1–3] The resulting Rh^{II}-carbene is capable of a wide range of reactions including C–H and X–H (X = O, N, S, Si, B) insertion reactions, ylide transformations, and cyclopropanation, which have made it a versatile synthetic tool.[3–9] Despite their wide utility, a common problem is the formation of side products due to competitive carbene dimerisation (homocoupling).[10,11] Carbenoids derived from ethyl diazoacetate (EDA) are particularly prone to side products derived from carbene dimerisation[12,13] and a well-used strategy to suppress dimer formation is to use an excess, typically 5–10 equivalents, of the substrate. This method can be problematic, however, in cases where precious substrates or late-stage applications are concerned.[14]

While bridging ligand design is a major focus in the development of Rh^{II} complexes,[2,15–23] we hypothesised that axial sites on the complex can be used to modulate Rh-carbene reactivity such that side products due to dimerisation could be minimised. Early studies of the axial sites of Rh^{II} complexes focused on the role of solvents and other Lewis bases and their effect on the Rh–Rh bond.[24–26] It was observed that coordination to the axial site occurs sequentially wherein the first equivalent binds stronger than the second due to the cooperative ability of the two Rh atoms.[27] Applying these fundamental studies to benefit catalytic performance has been somewhat ambiguous but has received attention as an alternative method for tuning Rh^{II} catalysts.[28] It was clear that solvents such as acetonitrile (MeCN) decreased yields in catalytic applications by binding to the axial site and inhibiting catalysis.[24,29,30] There are situations, though, in which Lewis base additives have improved yields[31,32] and selectivity[33–35] in diazo-mediated reactions. In these instances, axial coordination of the additives was believed to be playing a role. The addition of exogenous ligands, however, is complicated by the inherent weakness of axial site coordination of neutral donors.

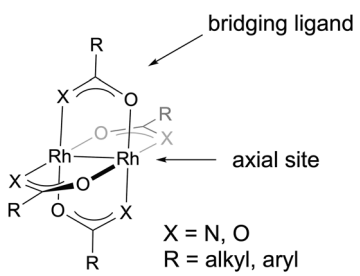

Fig. 1 General structure of Rh^{II} carboxylate (X = O) and carboxamidate (X = N) complexes.

Department of Chemistry, University of Tennessee, Knoxville, TN 37796-1600, USA. E-mail: adarko@utk.edu

†Electronic supplementary information (ESI) available: Experimental procedures, X-ray crystal data, cyclic voltammetry, computational data, and NMR spectra. CCDC 2021387. For ESI and crystallographic data in CIF or other electronic format see DOI: 10.1039/d0dt03019h

As a result, the coordination exists in solution as an equilibrium, leading to uncertainty as to whether axial coordination is involved in the catalytically active species.[36] One strategy to circumvent the issue is to add a large excess of additive to increase the probability of axial coordination during catalysis.[37] Another method that has been explored is to implement a strong σ donor, such as N-heterocyclic carbenes,[38,39] that will irreversibly bind to the axial site. Both of these strategies often lead to decreased catalyst performance or result in only marginal benefits in Rh^{II}-carbene reactions.

To better utilise and enhance the effect of axial coordination on Rh^{II} complexes, we have developed bridging ligands with tethered thioether moieties that are capable of axial coordination. Incorporation of a tether increases the local concentration of the axial coordinating group and gives significantly more control over the coordination to the axial site. The ligand design was inspired by similar scaffolds reported by Bera[40] and Ball,[41] in which tethered axial coordination resulted in interesting results in α-diazocarbonyl mediated C–H insertion and cyclopropanation. Initial reports of our bespoke Rh^{II} complexes proved that they were proficient in cyclopropanation[42] and Si–H insertion reactions[43] with donor/acceptor carbenes (Chart 1). Most importantly, we demonstrated that dimerisation could be minimised by incorporating tethered, axially coordinated thioether groups. In the examples where cyclopropanation was concerned, excess substrate was required for adequate yields. Charette and co-workers were able to obtain good yields with 2 equivalents of alkene using conventional Rh^{II} complexes in a biphasic system,[44] but reports of good yields using equimolar alkene to diazo in Rh^{II}-mediated intermolecular cyclopropanation reactions remain scarce.[9] To address this gap, we sought to fine-tune catalyst performance by varying tether lengths and thioether substituents on our oxazolidinone-based scaffold. Herein, we report the microwave-assisted synthesis of heteroleptic Rh^{II} complexes comprised of oxazolidinone bridging ligands equipped with tethered thioether groups of varying tether lengths and substituents. The complexes were utilised to maximise yields in the cyclopropanation of alkenes with EDA. Further analysis of the complexes by UV-Vis, cyclic voltammetry, and computational chemistry was conducted to explain the observed reactivity.

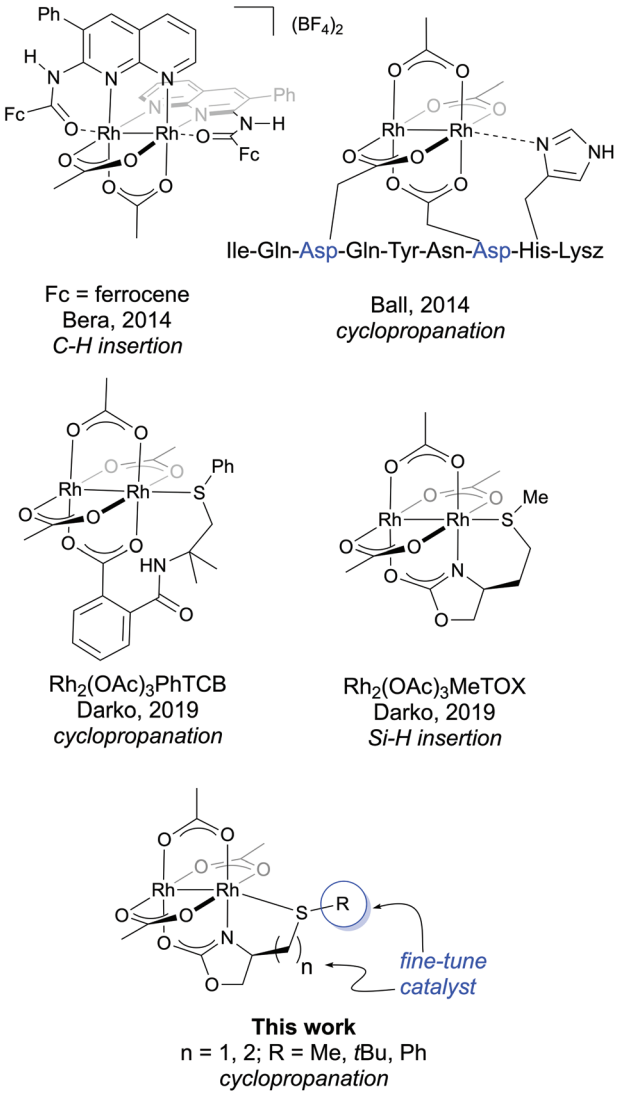

Chart 1 Dirhodium complexes with tethered, axial coordination in diazo-mediated applications.

2. Results and discussion

A challenge for the study of our axially coordinated catalysts is the need to synthesize heteroleptic complexes. Traditionally, homoleptic complexes are obtained through sequential substitution of the acetate bridging ligands of dirhodium acetate with the desired ligand.[11] Full ligand substitution is driven by the removal of displaced acetate through trapping methods. When using this strategy to produce heteroleptic complexes, results are hampered by a complex statistical mixture of products.[22,23] Alternatively, one can start with a dirhodium precursor with bridging ligands of varying aptitude for dissociation.[45,46] Corey used this method to synthesize heteroleptic imidazolidinate complexes, however, the number of isomers was further complicated by the orientation of the N and O atoms around each Rh atom.[46,47] We observed that the incorporation of the thioethers on our ligand scaffold significantly reduced the number of products in heteroleptic complex synthesis.[42] Each ligand substitution either slowed or blocked further ligand substitution such that only products from mono- and bis-tethered adducts were produced. Reaction times were a bit sluggish in the case of the oxazolidinate scaffold, so we turned to microwave synthesis to accelerate the process.

Microwave conditions have previously been implemented for expediting the synthesis of homoleptic dirhodium paddlewheel complexes,[48,49] and we were attracted to the microwave synthesis of each complex, even in small amounts, to facilitate rapid access to a range of catalysts for reaction studies. The

synthesis of catalyst **2**[42] and **3** from ligand **1a** and rhodium acetate was used for initial optimisation studies. Product formation was initially observed in low yields at 160 °C (Table 1, entry 2). Prolonged time at 160 °C did not dramatically improve yields (Table 1, entries 3 and 4). Increased temperatures led to an increase in complexes **2** and **3**, with preferred formation of **2** (Table 1, entry 5). A series of solvents with varied coordinating ability were then screened (Table 1, entries 5–9). Ethanol gave a high per cent conversion (Table 1, entry 7) but provided low yields of **2** and **3** along with the presence of a grey solid. It has been reported that ethanol facilitates the reduction of Rh^{II} to Rh metal, which would explain the grey solid residue in the reaction vessel.[50] As observed with other ligand exchange conditions, the weakly coordinating solvents 1,2-dichloroethane (DCE) and chlorobenzene (PhCl) produced the highest yields (Table 1, entries 5 and 9). Although they gave similar yields, DCE was used in further reactions due to its convenience in reaction workup. A further increase in temperature to 190 °C afforded the optimal conversion and product yield while producing the desired mono-complex **2** preferentially to the bis-complexes **3a** and **3b** (Table 1, entry 10). Continuing to increase the temperature did not significantly improve yields (Table 1, entry 11).

Other oxazolidinone ligands were synthesized from serine and aspartic acid, providing tether lengths of one and two methylene units, respectively (**1b–d**, Fig. 2). Ligand exchange reactions using the optimised microwave conditions furnished complexes **2–9** (Fig. 2). The mono-substituted complexes formed preferentially in all cases, but the ratio of mono-to-bis increased according to donating strength of the thioether substituent. More specifically, the stronger donating *t*-butyl group

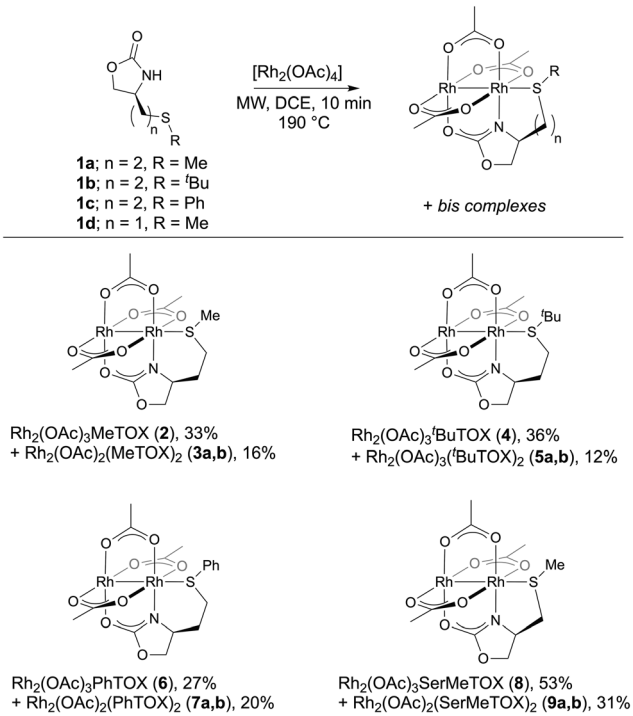

Fig. 2 Complexes synthesized *via* microwave method.

in ligand **1b** furnished a 3 : 1 ratio of complexes **4** to **5** compared with 1.3 : 1 for **6** to **7**, in which the sulphur substituent was phenyl. Higher overall yields were obtained when the tether length was one methylene unit compared to two methylene units, as evidenced by comparing yields of complexes from ligand **1a** to those from ligand **1d**. It is worthy to note that while ligands with pendant thioethers proceeded readily with one equivalent of the ligand under microwave conditions, synthesis of mixed ligand oxazolidinate/carboxylate complexes without axial coordination required excess ligand to drive the reaction forward,[43,46] suggesting that the tethered thioether facilitates ligand exchange.

We have previously reported the X-ray structure for complex **2**,[42] and we were able to obtain suitable crystals for X-ray analysis for complex **6** *via* slow evaporation of a 1 : 1 mixture of acetonitrile and toluene (Fig. 3). Despite our efforts, we were unable to obtain X-ray quality crystals of the other new complexes. Unlike complex **2**, $Rh_2(OAc)_3$PhTOX (**6**) does not form an oligomeric chain in the solid state. Instead, the asymmetric unit is comprised of four distinct paddlewheel units in which the second axial site is occupied by acetonitrile (see ESI†). A stereogenic centre is created at the sulphur atom upon coordination to the Rh centre.[51–54] As a result, a mixture of diastereomers are present, (S_C, R_S) and (S_C, S_S), due to the sulphur stereogenic centre and the *S* configuration at the asymmetric carbon on the bridging oxazolidinate (Fig. 3). Of the four paddlewheel units, two are (S_C, R_S) and two structures are (S_C, S_S), with minor structural variations between them. Representatives of each pair are shown in Fig. 3. The Rh–Rh bond distances for each paddlewheel unit does not vary

Table 1 Optimization of microwave synthesis parameters for Rh^{II} complex synthesis

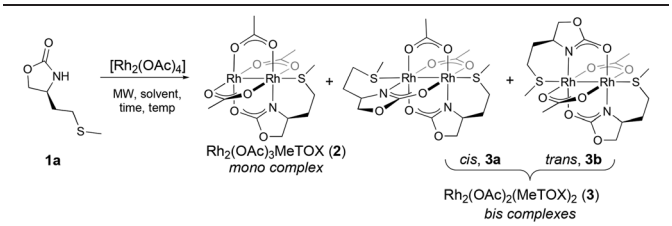

Entry	Solvent	Time (min)	Temp. (°C)	Yield[a] **2** (%)	Yield[a] **3a**, **b** (%)	Conv.[a] (%)
1	DCE	10	140	1	0	3
2	DCE	10	160	6	1	7
3	DCE	20	160	13	3	18
4	DCE	30	160	17	5	23
5	DCE	10	180	22	7	46
6	THF	10	180	4	2	9
7	EtOH	10	180	14	7	79
8	MeCN	10	180	18	5	29
9	PhCl	10	180	21	5	27
10	**DCE**	**10**	**190**	**33**	**16**	**52**
11	DCE	10	200	33	17	53

[a] Yield and conversion determined by HPLC.

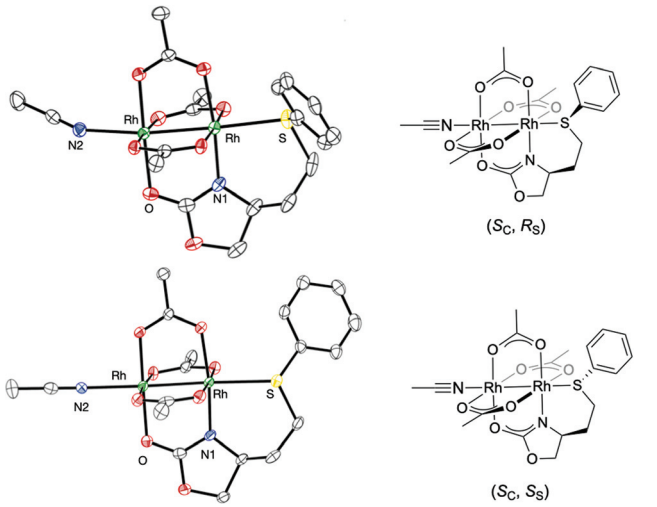

Fig. 3 X-Ray structure of complex **6** with thermal ellipsoids at 50% probability. Only two of the four molecules in the asymmetric unit is shown. Selected bond lengths and angles as an average of the four structures of the asymmetric unit: Rh–Rh 2.42 Å, Rh–S 2.50 Å, Rh–N2 2.24 Å, Rh–Rh–S 175.5°.

(average of 2.4217(5) Å) and is within the general range for Rh–Rh bonds in paddlewheel complexes, which are typically between 2.35–2.45 Å.[55] The Rh–S bond distances of complex **6** range between 2.4730(12)–2.5195(12) Å. The observation that the Rh–S bonds are not constant suggests that the phenyl thioether axial ligand is in a fluxional state and is a weaker donor than the methyl sulphide in **2**, in which the intramolecular Rh–S bond is 2.48 Å.[42] The Rh–N2 bond distance varies little and averages 2.236(4) Å between the paddlewheel structures, but pairs of the structures have differences in Rh–Rh–N angles. The (S_C, R_S) pair has slightly bent Rh–Rh–N angles of 171°, while the (S_C, S_S) pair has almost linear Rh–Rh–N angles of 175°. The variations are most likely a consequence of packing effects, but they give insight into the structural flexibility of the complex.

In general, axially coordinated molecules bind to the σ* orbital of the Rh–Rh centre, which perturbs the π* to σ* HOMO–LUMO gap. This is manifested by shifts in the visible region of their UV-vis spectrum.[56] Fig. 4 shows the overlaid UV-vis spectra of the mono-complexes **2**, **4**, **6**, and **8**. The colours of the mono-complexes are shades of violet and the local maxima of their bands in the visible region are clustered between 572 nm to 582 nm. The similarity between them suggests that varying the tether length (between 1 or 2 methylene units) or varying the thioether substituent (Me, ^{t}Bu, or Ph) does not significantly alter the HOMO–LUMO energy gap of the complex (Fig. 4).

We initially explored the reactivity of the various rhodium catalysts in the cyclopropanation of styrene with ethyl diazoacetate (EDA) using optimal conditions from our previous studies.[42] We anticipated that performing the reactions with excess styrene would likely result in high yields of the cyclopropane product for most of the catalysts. Therefore, to better distinguish the performance of the catalysts, reactions were conducted with equimolar amounts of styrene to EDA. In this way, selectivity between carbene dimerisation and cyclopropanation could be evaluated. In contrast to previous work in our group demonstrating low reactivity for catalyst **2** with donor/acceptor diazo compounds in the cyclopropanation of styrene,[42] it was a very competent catalyst when EDA was used, providing 63% yield of cyclopropane **10** and trace yields of dimer products (Table 2, entry 1). The length of the tether only had a minor influence on the yield of **10**, but the change resulted in increased dimer formation (Table 2, compare entries 1 and 2). The thioether substituent had a more pronounced effect on cyclopropane yield. Complex **6**, with a phenyl substituent on the thioether, provided the highest cyclopropane yield of the series (71%, Table 2, entry 3), while the complexes with alkyl substituents on the thioether (complexes **2**, **4**, and **8**) gave

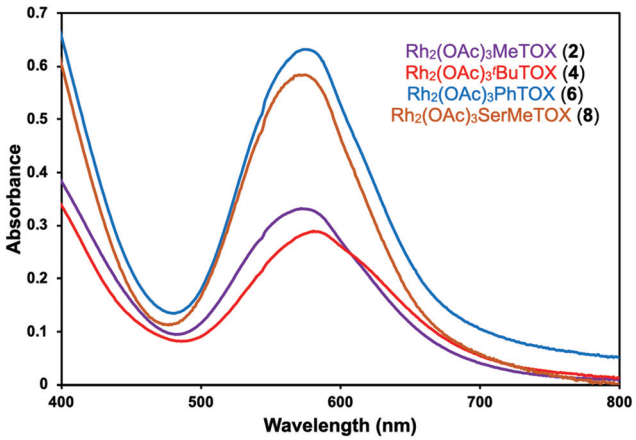

Fig. 4 UV-vis spectrum of complexes **2**, **4**, **6**, and **8**.

Table 2 Catalyst screening for the cyclopropanation of styrene with ethyl diazoacetate

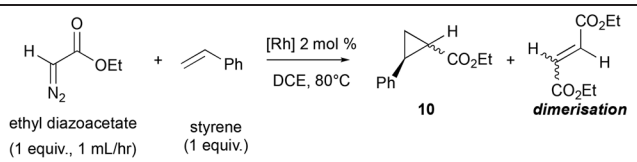

Entry	[Rh]	Yield **10**[a] (%)	Yield **dimer** (%)
1	**2**	63	<1
2	**8**	59	8
3	**6**	71	<1
4	**4**	57	<1
5	$Rh_2(OAc)_4$	33	3
6	$Rh_2(OAc)_3OX$	38	3
7	**3a,b**	19	8
8[b]	**6**	62	1
9[b]	$Rh_2(OAc)_3OX$	36	11
10[c]	**6**	53	3
11[c]	$Rh_2(OAc)_3OX$	30	17

[a] Yields determined by GC and averaged over 2 runs. [b] 1 mol% catalyst. [c] 0.1 mol% catalyst.

essentially comparable yields (Table 2, entries 1–4). Except for complex **8**, the mono-substituted tethered complexes had only trace amounts of dimer products. All of the tethered complexes outperformed dirhodium tetraacetate in cyclopropane yield (Table 2, entry 5). $Rh_2(OAc)_3OX$ was also tested to eliminate the possibility that the bridging oxazolidinate ligand was responsible for the yield increases. However, $Rh_2(OAc)_3OX$ also obtained cyclopropane **10** in a lower yield compared to the tethered complexes, further implicating the tethered thioether as the reason for increased yields (Table 2, entry 6). As observed in our previous work, the mixed bis-substituted complexes **3a**,**b** exhibited greatly diminished catalytic activity (Table 2, entry 7).[42,43] In this reaction, some carbene dimerisation was observed along with a high percentage of unreacted EDA. The dual tether of the bis-complex likely blocks both axial sites, requiring displacement before catalysis is possible and thereby reducing reaction yield. Dimerisation yields were more of an issue for non-tethered complexes when catalyst loading was reduced, but the side product was kept minimal when complex **6** was used, although a drop in cyclopropanation yield was observed (Table 2 entries 8–11). At 0.1 mol% of catalyst, complex **6** provided a 53% yield of **10** with 3% of the dimer products, while $Rh_2(OAc)_3OX$ gave a 30% yield of **10** and 17% yield of dimer products (Table 2 entry 10 and 11). This result is evidence that the thioether tether may assist with catalyst turnover, an issue that is present when ethyldiazo acetate is used as the diazo precursor.[57]

A substrate scope was conducted for the cyclopropanation reaction using 2 mol% of complex **6** (Fig. 5). Styrene derivatives **10–14** generally maintained good yields at 1 equivalent of olefin and high yields of cyclopropane when 5 equivalents were used. 4-*t*-Butylstyrene provided similar yields of product **12** compared to styrene, while 4-chlorostyrene gave a slightly lower yield of compound **11**. This is consistent with inductive withdrawing effects of the Cl resulting in a less nucleophilic olefin. Introduction of steric hindrance *via* disubstituted olefins also resulted in good to excellent yields, albeit slightly lower than monosubstituted olefins (**13** and **14**, Fig. 5). Non-styrene derivatives **15** and **16** performed well in the reaction when 5 equivalents of olefin were used. Using 5 equivalents of the electron-rich ethyl vinyl ether afforded quantitative amounts of cyclopropane **15**, but only 31% yield at 1 equivalent. We hypothesized that volatility of the vinyl ether was partly to blame for the low yield. Performing the experiment at room temperature slightly increased the yield to a 43% yield of **15**. The synthetically challenging norbornene afforded moderate yields of its respective cyclopropane (compound **16**) at 5 equivalents, but low yield at 1 equivalent. In all cases, the diastereomeric ratio of the cyclopropanes did not differ markedly from that observed in the literature.[58] This was anticipated as EDA generally gives low diastereoselectivities in Rh^{II}-carbene cyclopropanation reactions (Fig. 5).[59–61]

Cyclic voltammetry experiments were performed to probe the effect of the tethered thioether ligands on the electronics at the Rh metal centres. Early studies demonstrated that the variance of the $Rh_2^{4+/5+}$ oxidation potential could be used as a

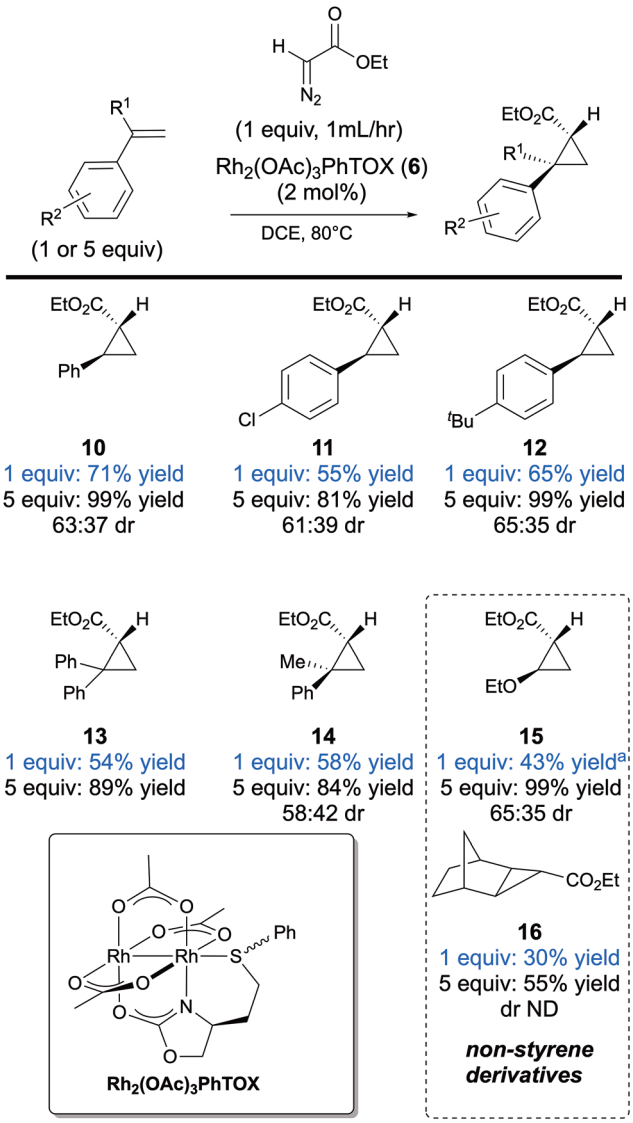

Fig. 5 $Rh_2(OAc)_3PhTOX$-catalyzed cyclopropanation with ethyl diazoacetate. Yields are averaged over 2 runs and calculated by ^{1}HNMR except for compounds **10** and **15**. [a] Performed at 25 °C.

metric for the strength of axial coordination.[29] Our analysis was conducted in 0.1 M [TBA][PF_6] in dichloromethane. Fig. 6 is a stack of the cyclic voltammograms of the Rh^{II} complexes. Each of the complexes displayed a reversible, or quasi-reversible, oxidation event assigned to the $Rh_2^{4+/5+}$ couple. Oxidation potentials of the mono-complexes followed the trend that increased σ donating ability of the tethered thioether corresponded to a higher oxidation potential (Fig. 6). This is contrary to previous studies in which the sequential addition of exogenous axial ligands resulted in a lower oxidation potential.[30] This increased oxidation potential, though unexpected, is not unprecedented. We have shown this trend to be the case with respect to $Rh_2(OAc)_3PhTCB$ complexes (PhTCB = phenylthiocarbamoyl benzoate), which also contains a tethered thioether and showed a $Rh_2^{4+/5+}$ $E_{1/2}$ value 36 mV higher than

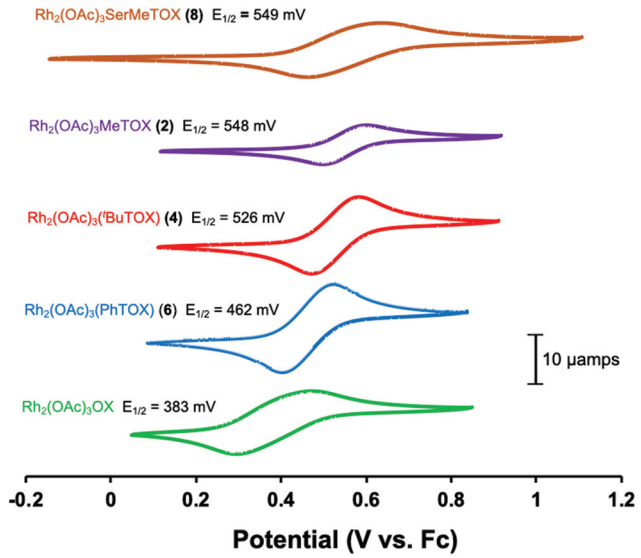

Fig. 6 Cyclic voltammograms of complexes **2**, **4**, **6**, **8**, and $Rh_2(OAc)_3OX$. Electrolyte comprised of 0.1 M [TBA][PF_6] in DCM (scan rate of 100 mV s^{-1}).

$Rh_2(OAc)_3OBz$ (OBz = benzoate).[42] It is worth noting that the same trend was not observed when the CV experiments of complexes **2**, **4**, **6**, and **8** were conducted in MeCN, confirming that the electrochemical study of the complexes is sensitive to coordinating solvents (see ESI†).

DFT calculations were employed as a means of further understanding the electronic structure of the complexes. Theoretical calculations of the precursor complexes, as well as their carbene complexes with EDA, were calculated at the MO6-2X/def2-TZVPP level of theory. According to Berry's three centre/four electron (3c/4e) bonding model, the addition of axial ligands has the most impact in the energy of the Rh–Rh σ* orbital, which is the LUMO of the complex.[56] The out-of-phase combination of the axial ligand's lone pair σ orbitals interact with the Rh–Rh σ* orbital and raise the energy of the Rh–Rh σ* LUMO. When comparing complex **6** to $Rh_2(OAc)_3OX$, the most dramatic change was in the destabilisation of the Rh–Rh σ* LUMO due to their interaction with the thioether lone pairs (Fig. 7). The extent of destabilisation is greater with **2**[43] than **6**, hence, stronger axial interactions lead to greater destabilisation, which is in agreement with the 3c/4e model.[56,62] The effect of the axial ligands also raises the energy of the Rh–Rh π* HOMO, but this energy destabilisation is minor compared to that of the LUMO. The combined effects lead to larger HOMO–LUMO gaps for the complexes with tethered thioethers when compared to $Rh_2(OAc)_3OX$.

Upon analysis of the LUMO of the carbene species, we found interesting differences in the electronic structure of the tethered complexes (Fig. 8). The LUMO of Rh-carbene **17** comprises of an interaction of the p orbital of the carbene with a filled Rh–Rh π* orbital, which is normally the case with axially free rhodium complexes.[63] The extent of π backbonding decreases the electrophilicity of the carbene, but this interaction is polarized towards the Rh, leading to "super electrophilic" carbenes.[56,64] In the case of the tethered thioether carbene complex **18**, the LUMO seems to include a mixed electronic environment at the Rh core—π symmetry at the Rh–C and σ symmetry at the Rh–S. Such mixing of σ and π components in metal–metal bonding has been reported for trir-

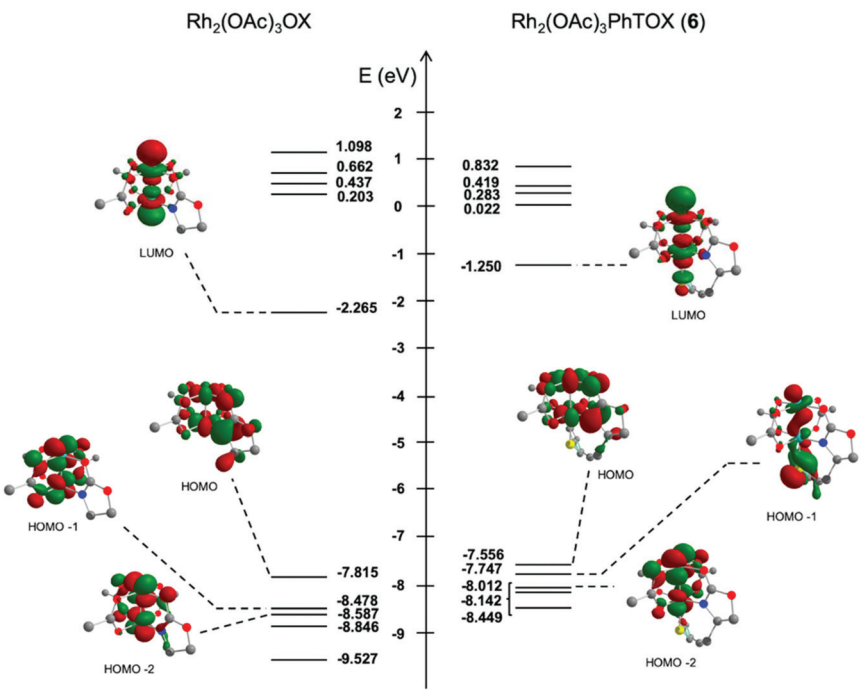

Fig. 7 Molecular orbitals of complex **6** in comparison to $Rh_2(OAc)_3OX$ calculated at the MO6-2X/def2-TZVPP level of theory.

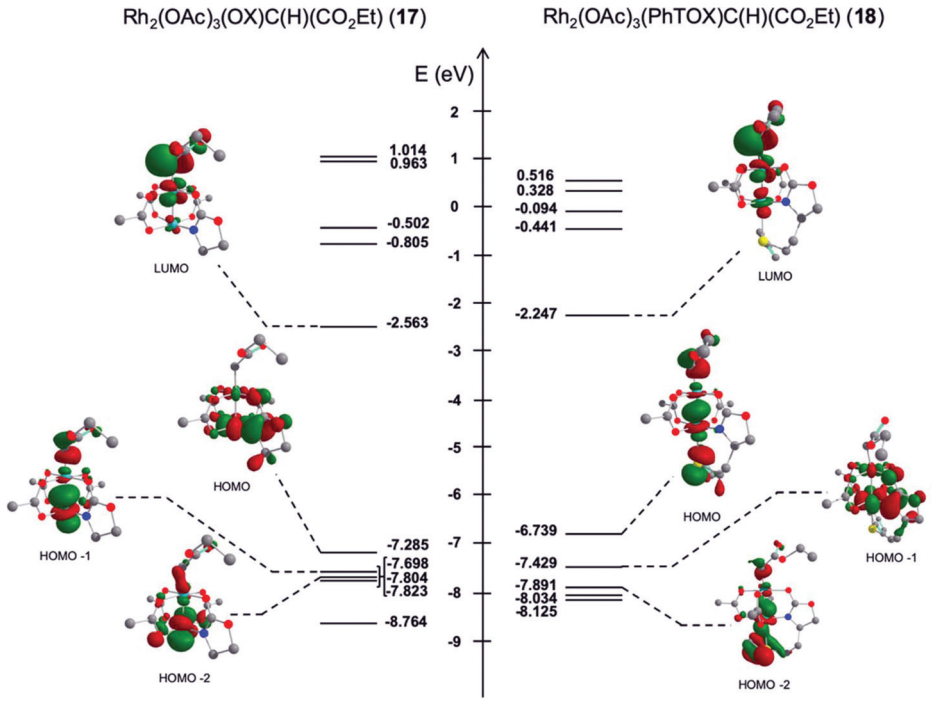

Fig. 8 Calculated orbitals and energies of EDA carbenoid species **17** and **18**. Calculated at the MO6-2X/def2-TZVPP level of theory.

uthenium extended metal-atom chains (EMACs) in which bending of the linear structure introduces mixing of σ and π orbitals in the Ru_3 core.[65] In our case, the calculated S–Rh–Rh (176°) and Rh–Rh–C (168°) angles in **18** deviate from linearity compared to **17** (Rh–Rh–C ~177°) and this reduction in symmetry may be the driving force for the interaction of the σ and π orbitals. A result of this distortion is an increase in the energy of the LUMO orbital of **18** compared to **17**. Although this is not a dramatic increase in energy (0.316 eV or 7.29 kcal mol^{-1}), it opens the possibility of further perturbing the Rh^{II}-carbene LUMO energy with distal axial coordination.

The more significant energy destabilisation occurs in the HOMO of the carbene complexes with tethered thioether ligands. The HOMO of the carbene from tethered complex **18** is comprised of a Rh–Rh σ-bonding orbital with significant carbene character. Out-of-phase σ interactions characterize both the interaction of the tethered thioether and carbene with the Rh centre. In contrast, in the untethered complex **17**, the HOMO is a Rh–Rh π* orbital with no carbene character. It is plausible that the difference in the HOMOs is an important factor in the enhanced reactivity of the complexes with tethered thioether ligands. A similar change in the electronic character of the HOMO was observed when carboxylate paddlewheel complexes with Rh–Rh and Rh–Bi metal centres were compared. Fürstner and co-workers observed extreme electrophilicity of Rh–Bi acceptor carbene complexes and implicated 3c/4e interactions in the σ framework as the major contributor.[64] Davies and co-workers also observed similar qualitative orbital topologies with Rh–Bi donor/acceptor carbene complexes and proposed that the HOMO of the Rh–Bi complex should result in a more nucleophilic carbenoid.[66] It is generally accepted that cyclopropanation occurs *via* a concerted, but asynchronous process that is initiated by nucleophilic attack on the carbene carbon by the olefin.[67] We speculate that since the HOMO of the tethered complexes partially lies on the carbene carbon, it could more readily facilitate the formation of the cyclopropane ring over other competing pathways.

Further support for σ interactions in the HOMO as a major factor is provided by the calculated bond distances for the carbene species, in which the tethered complex **18** possesses an elongated Rh–C bond in comparison to the untethered carbene complex **17** (Table 3). Natural population analysis of

Table 3 Calculated geometric parameters and NBO analysis of **17** and **18**. Calculated at the MO6-2X/def2-TZVPP level of theory

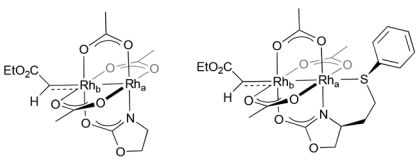

17 **18**

Natural Population Analysis			Bond distances (Å)		
	17	**18**		**17**	**18**
Rh_a	0.523	0.407	Rh_a–Rh_b	2.47	2.45
Rh_b	0.625	0.592	Rh_b–$C_{carbene}$	1.86	1.91
$C_{carbene}$	0.174	0.095	Rh_a–S	—	2.76
S	—	0.394			

the carbene complexes shows increased electron density at the carbene carbon of **18** compared to **17** (0.095 *vs.* 0.174 respectively, Table 3), meaning that the tethered thioether is capable of modulating the electron density at the distal carbene. This remote modulation of electron density could account for the reactivity and also be a factor in reducing the barrier for the rate-limiting diazo extrusion step,[67,68] thereby increasing catalyst turnover. Theoretical calculations are underway to better address the effects of tethered ligands on transition states and energy barriers in diazo-mediated transformations.

3. Conclusions

In conclusion, heteroleptic dirhodium(II) paddlewheel complexes containing axially coordinated thioether ligands were synthesized using a microwave-assisted approach. We have demonstrated that catalyst synthesis and reactivity is influenced by the tether length and the substituent of the thioether. The tethered complexes achieved higher yields that their non-tethered counterparts in the cyclopropanation of styrene with ethyl diazoacetate, even demonstrating good yields with equimolar amounts of styrene substrate. Electronic studies and computational methods provided insight into the effect of the donating strength of the tethered ligands on the observed reactivity. The calculations were of particular relevance, revealing the importance of the effect of the tethered thioether on the HOMO of the Rh^{II}-carbene complexes. Efforts to further understand the interplay between the donor of the tether and reactivity in Rh^{II}-carbene mediated reactions are currently ongoing.

Conflicts of interest

There are no conflicts to declare.

Acknowledgements

We are grateful for financial support from the University of Tennessee Knoxville in Knoxville, TN. We thank John F. Berry (University of Wisconsin–Madison) for useful discussions concerning the electronic structure calculations. We also thank the personnel in the NMR, Biological and Small Molecule Mass Spectrometry Core, and analytical facilities at the University of Tennessee. We also wish to thank Prof. David Jenkins for facilitating our electrochemical experiments.

References

1 M. P. Doyle and D. C. Forbes, *Chem. Rev.*, 1998, **98**, 911–935.
2 M. P. Doyle, *J. Org. Chem.*, 2006, **71**, 9253–9260.
3 R. Paulissen, H. Reimlinger, E. Hayez, A. J. Hubert and P. Teyssié, *Tetrahedron Lett.*, 1973, **14**, 2233–2236.
4 H. Keipour, V. Carreras and T. Ollevier, *Org. Biomol. Chem.*, 2017, **15**, 5441–5456.
5 H. M. L. Davies and D. Morton, *Chem. Soc. Rev.*, 2011, **40**, 1857–1869.
6 K. M. Chepiga, C. M. Qin, J. S. Alford, S. Chennamadhavuni, T. M. Gregg, J. P. Olson and H. M. L. Davies, *Tetrahedron*, 2013, **69**, 5765–5771.
7 D. Gillingham and N. Fei, *Chem. Soc. Rev.*, 2013, **42**, 4918–4931.
8 Y. Pang, Q. He, Z.-Q. Li, J.-M. Yang, J.-H. Yu, S.-F. Zhu and Q.-L. Zhou, *J. Am. Chem. Soc.*, 2018, **140**, 10663–10668.
9 H. M. L. Davies and E. G. Antoulinakis, *Org. React.*, 2001, **57**, 1–326.
10 J. H. Hansen, B. T. Parr, P. Pelphrey, Q. Jin, J. Autschbach and H. M. L. Davies, *Angew. Chem., Int. Ed.*, 2011, **50**, 2544–2548.
11 M. P. Doyle, M. A. McKervey and T. Ye, *Modern Catalytic Methods for Organic Synthesis with Diazo Compounds: from Cyclopropanes to Ylides*, Wiley, New York, 1998.
12 H. M. L. Davies, L. M. Hodges, J. J. Matasi, T. Hansen and D. G. Stafford, *Tetrahedron Lett.*, 1998, **39**, 4417–4420.
13 I. Dragutan, V. Dragutan and F. Verpoort, *Appl. Organomet. Chem.*, 2014, **28**, 211–215.
14 X. Liu, J. Liu, J. Zhao, S. Li and C.-C. Li, *Org. Lett.*, 2017, **19**, 2742–2745.
15 Y. Deng, H. Qiu, H. D. Srinivas and M. P. Doyle, *Curr. Org. Chem.*, 2016, **20**, 61–81.
16 H. M. L. Davies and B. T. Parr, in *Contemporary Carbene Chemistry*, ed. R. A. Moss and M. P. Doyle, John Wiley & Sons, Inc, Hoboken, New Jersey, 2013, vol. 7, pp. 363–403.
17 C. Qin and H. M. L. Davies, *J. Am. Chem. Soc.*, 2014, **136**, 9792–9796.
18 F. G. Adly, *Catalysts*, 2017, **7**, 347.
19 S. Miah, A. M. Z. Slawin, C. J. Moody, S. M. Sheehan, J. P. Marino, M. A. Semones, A. Padwa and I. C. Richards, *Tetrahedron*, 1996, **52**, 2489–2514.
20 P. Panne and J. M. Fox, *J. Am. Chem. Soc.*, 2007, **129**, 22–23.
21 D. F. Taber, R. P. Meagley, J. P. Louey and A. L. Rheingold, *Inorg. Chim. Acta*, 1995, **239**, 25–28.
22 V. N. G. Lindsay and A. B. Charette, *ACS Catal.*, 2012, **2**, 1221–1225.
23 D. T. Boruta, O. Dmitrenko, G. P. A. Yap and J. M. Fox, *Chem. Sci.*, 2012, **3**, 1589–1593.
24 R. S. Drago, J. R. Long and R. Cosmano, *Inorg. Chem.*, 1981, **20**, 2920–2927.
25 R. S. Drago, J. R. Long and R. Cosmano, *Inorg. Chem.*, 1982, **21**, 2196–2202.
26 C. Bilgrien, R. S. Drago, G. C. Vogel and J. Stahlbush, *Inorg. Chem.*, 1986, **25**, 2864–2866.
27 R. S. Drago, S. P. Tanner, R. M. Richman and J. R. Long, *J. Am. Chem. Soc.*, 1979, **101**, 2897–2903.
28 A. F. Trindade, J. A. S. Coelho, C. A. M. Afonso, L. F. Veiros and P. M. P. Gois, *ACS Catal.*, 2012, **2**, 370–383.
29 K. Das, K. M. Kadish and J. L. Bear, *Inorg. Chem.*, 1978, **17**, 930–934.

30 M. Y. Chavan, T. P. Zhu, X. Q. Lin, M. Q. Ahsan, J. L. Bear and K. M. Kadish, *Inorg. Chem.*, 1984, **23**, 4538–4545.
31 T. D. Nelson, Z. J. Song, A. S. Thompson, M. Z. Zhao, A. DeMarco, R. A. Reamer, M. F. Huntington, E. J. J. Grabowski and P. J. Reider, *Tetrahedron Lett.*, 2000, **41**, 1877–1881.
32 H. M. L. Davies and A. M. Walji, *Org. Lett.*, 2003, **5**, 479–482.
33 D. Marcoux, V. N. G. Lindsay and A. B. Charette, *Chem. Commun.*, 2010, **46**, 910–912.
34 V. N. G. Lindsay, C. Nicolas and A. B. Charette, *J. Am. Chem. Soc.*, 2011, **133**, 8972–8981.
35 S. C. Martin, F. Vohidov, H. P. Wang, S. E. Knudsen, A. A. Marzec and Z. T. Ball, *Bioconjugate Chem.*, 2017, **28**, 659–665.
36 A. N. Zaykov and Z. T. Ball, *Tetrahedron*, 2011, **67**, 4397–4401.
37 D. Poggiali, A. Homberg, T. Lathion, C. Piguet and J. Lacour, *ACS Catal.*, 2016, **6**, 4877–4881.
38 L. F. R. Gomes, A. F. Trindade, N. R. Candeias, L. F. Veiros, P. M. P. Gois and C. A. M. Afonso, *Synthesis*, 2009, 3519–3526.
39 L. F. R. Gomes, A. F. Trindade, N. R. Candeias, P. M. P. Gois and C. A. M. Afonso, *Tetrahedron Lett.*, 2008, **49**, 7372–7375.
40 M. Sarkar, P. Daw, T. Ghatak and J. K. Bera, *Chem. – Eur. J.*, 2014, **20**, 16537–16549.
41 R. Sambasivan, W. Zheng, S. J. Burya, B. V. Popp, C. Turro, C. Clementi and Z. T. Ball, *Chem. Sci.*, 2014, **5**, 1401–1407.
42 B. G. Anderson, D. Cressy, J. J. Patel, C. F. Harris, G. P. A. Yap, J. F. Berry and A. Darko, *Inorg. Chem.*, 2019, **58**, 1728–1732.
43 W. Sheffield, A. Abshire and A. Darko, *Eur. J. Org. Chem.*, 2019, 6347–6351.
44 R. P. Wurz and A. B. Charette, *Org. Lett.*, 2002, **4**, 4531–4533.
45 S. C. Martin, M. B. Minus and Z. T. Ball, *Methods Enzymol.*, 2016, **580**, 1–19.
46 Y. Lou, T. P. Remarchuk and E. J. Corey, *J. Am. Chem. Soc.*, 2005, **127**, 14223–14230.
47 M. P. Doyle, C. E. Raab, G. H. P. Roos, V. Lynch and S. H. Simonsen, *Inorg. Chim. Acta*, 1997, **266**, 13–18.
48 O. F. Gonzalez-Belman, Y. Varela, M. Flores-lamo, K. Wrobel, S. Gutierrez-Granados, J. M. Peralta-Hernndez, J. O. C. Jimnez-Halla and O. Serrano, *Int. J. Inorg. Chem.*, 2017, 1–12.
49 G. F. Keaney and J. L. Wood, *Tetrahedron Lett.*, 2005, **46**, 4031–4034.
50 S. A. Johnson, H. R. Hunt and H. M. Neumann, *Inorg. Chem.*, 1963, **2**, 960–962.
51 M. M. Major, G. Rovid, S. Balogh, A. Benyei, G. Lendvay, D. Frigyes, J. Bakos and G. Farkas, *Appl. Organomet. Chem.*, 2019, **33**, 1–14.
52 D. H. Bao, H. L. Wu, C. L. Liu, J. H. Xie and Q. L. Zhou, *Angew. Chem., Int. Ed.*, 2015, **54**, 8791–8794.
53 M. J. Page, J. Wagler and B. A. Messerle, *Organometallics*, 2010, **29**, 3790–3798.
54 A. M. Masdeu-Bulto, M. Dieguez, E. Martin and M. Gomez, *Coord. Chem. Rev.*, 2003, **242**, 159–201.
55 F. A. Cotton, C. A. Murillo and R. A. Walton, *Multiple Bonds between Metal Atoms*, Springer Science and Business Media, New York, NY, 3rd edn., 2005.
56 J. F. Berry, *Dalton Trans.*, 2012, **41**, 700–713.
57 P. Pelphrey, J. Hansen and H. M. L. Davies, *Chem. Sci.*, 2010, **1**, 254–257.
58 H. M. L. Davies, in *Org. React.*, ed. L. R. Overman, John Wiley & Sons, 2001, ch. Intermolecular Metal-Catalyzed Carbenoid Cyclopropanations, vol. 57.
59 M. P. Doyle, M. Protopopova, P. Muller, D. Ene and E. A. Shapiro, *J. Am. Chem. Soc.*, 1994, **116**, 8492–8498.
60 N. Watanabe, H. Matsuda, H. Kuribayashi and S. Hashimoto, *Heterocycles*, 1996, **42**, 537–542.
61 M. Barberis, J. Perez-Prieto, P. Lahuerta and M. Sanau, *Chem. Commun.*, 2001, 439–440.
62 E. Warzecha, T. C. Berto and J. F. Berry, *Inorg. Chem.*, 2015, **54**, 8817–8824.
63 E. Nakamura, N. Yoshikai and M. Yamanaka, *J. Am. Chem. Soc.*, 2002, **124**, 7181–7192.
64 L. R. Collins, M. van Gastel, F. Neese and A. Fürstner, *J. Am. Chem. Soc.*, 2018, **140**, 13042–13055.
65 P. J. Mohan, V. P. Georgiev and J. E. McGrady, *Chem. Sci.*, 2012, **3**, 1319–1329.
66 Z. Ren, T. L. Sunderland, C. Tortoreto, T. Yang, J. F. Berry, D. G. Musaev and H. M. L. Davies, *ACS Catal.*, 2018, **8**, 10676–10682.
67 D. T. Nowlan, T. M. Gregg, H. M. L. Davies and D. A. Singleton, *J. Am. Chem. Soc.*, 2003, **125**, 15902–15911.
68 M. C. Pirrung, H. Liu and A. T. Morehead, *J. Am. Chem. Soc.*, 2002, **124**, 1014–1023.